

## Article

# Optimization of Electrospinning Parameters for Lower Molecular Weight Polymers: A Case Study on Polyvinylpyrrolidone

Fatima Tuz Zahra <sup>1,\*</sup>, Ying Zhang <sup>2</sup>, Adeolu Oluwaseun Ajayi <sup>3</sup>, Quincy Quick <sup>4</sup> and Richard Mu <sup>1,\*</sup><sup>1</sup> TIGER Institute, Tennessee State University, Nashville, TN 37209, USA<sup>2</sup> Center for Manufacturing Research, Tennessee Technological University, Cookeville, TN 38505, USA; yzhang@tntech.edu<sup>3</sup> Department of Industrial Engineering and Operations Research, Columbia University in the City of New York, New York, NY 10027, USA; aoa2160@columbia.edu<sup>4</sup> Department of Biological Sciences, Tennessee State University, Nashville, TN 37209, USA; qquick@tnstate.edu

\* Correspondence: zfatima56@gmail.com (F.T.Z.); rmu@tnstate.edu (R.M.); Tel.: +1-615-397-2805 (F.T.Z.); +1-615-519-3370 (R.M.)

**Abstract:** Polyvinylpyrrolidone (PVP) is a synthetic polymer that holds significance in various fields such as biomedical, medical, and electronics, due to its biocompatibility and exceptional dielectric properties. Electrospinning is the most commonly used tool to fabricate fibers because of its convenience and the wide choice of parameter optimization. Various parameters, including solution molarity, flow rate, voltage, needle gauge, and needle-to-collector distance, can be optimized to obtain the desired morphology of the fibers. Although PVP is commercially available in various molecular weights, PVP with a molecular weight of 130,000 g/mol is generally considered to be the easiest PVP to fabricate fibers with minimal challenges. However, the fiber diameter in this case is usually in the micron regime, which limits the utilization of PVP fibers in fields that require fiber diameters in the nano regime. Generally, PVP with a lower molecular weight, such as 10,000 g/mol and 55,000 g/mol, is known to present challenges in fiber preparation. In the current study, parameter optimization for PVP possessing molecular weights of 10,000 g/mol and 55,000 g/mol was carried out to obtain nanofibers. The electrospinning technique was utilized for fiber fabrication by optimizing the above-mentioned parameters. SEM analysis was performed to analyze the fiber morphology, and quantitative analysis was performed to correlate the effect of parameters on the fiber morphology. This research study will lead to various applications, such as drug encapsulation for sustained drug release and nanoparticles/nanotubes encapsulation for microwave absorption applications.

**Keywords:** Polyvinylpyrrolidone; low molecular weight; electrospinning; nanofibers; parameters optimization; quantitative analysis; morphology



**Citation:** Zahra, F.T.; Zhang, Y.; Ajayi, A.O.; Quick, Q.; Mu, R. Optimization of Electrospinning Parameters for Lower Molecular Weight Polymers: A Case Study on Polyvinylpyrrolidone. *Polymers* **2024**, *16*, 1217. <https://doi.org/10.3390/polym16091217>

Academic Editor: Zina Vuluga

Received: 28 March 2024

Revised: 22 April 2024

Accepted: 24 April 2024

Published: 26 April 2024



**Copyright:** © 2024 by the authors. Licensee MDPI, Basel, Switzerland. This article is an open access article distributed under the terms and conditions of the Creative Commons Attribution (CC BY) license (<https://creativecommons.org/licenses/by/4.0/>).

## 1. Introduction

The electrospinning technique is a versatile method for fabricating fibers from a broad range of polymers. This process offers a wide array of controllable parameters, including flow rate (measured in mL/h), applied voltage (kV), needle gauge (G), and the distance between the needle tip and the collector (cm), as depicted in Figure 1's schematic of the electrospinning setup.

To begin electrospinning, a polymer solution is loaded into a syringe (connected to a metal needle), which is then set to a specific flow rate. The needle is connected to a direct current (DC) voltage supply that applies a high voltage, while the collector is grounded at a designated distance from the needle tip. Upon applying the voltage, a phenomenon to form the Taylor cone occurs, generating a fine fiber jet that propels toward the grounded collector. The careful manipulation of these process parameters allows for the customization of fiber morphology to meet specific application needs. The formation of the Taylor cone is crucial for successful fiber production. Therefore, optimizing the electrospinning parameters, in

conjunction with the intrinsic properties of the polymer solution—such as its volatility, viscosity, and conductivity—is essential. These properties not only influence the ability to form a Taylor cone but also affect the fiber morphology [1].

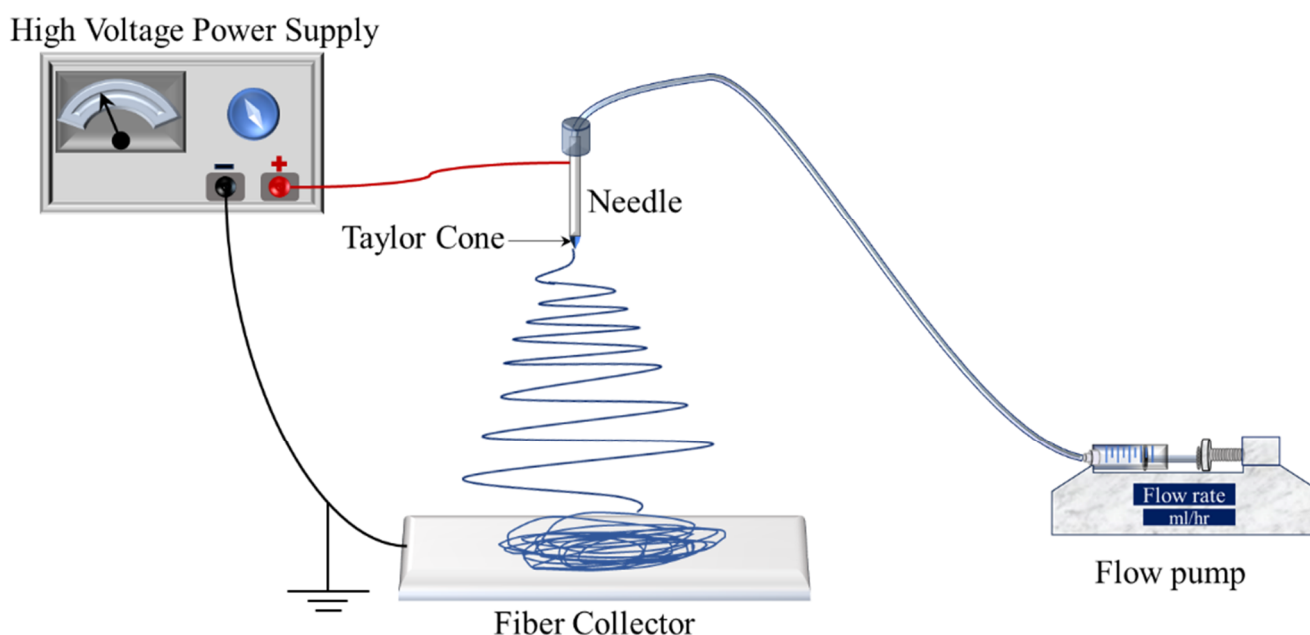


**Figure 1.** Schematic of electrospinning process.

Ambient conditions, including temperature and humidity, also play a significant role in determining fiber morphology. The choice of solvent for the polymer solution impacts its volatility; this is particularly important in biomedical applications like drug delivery, where a non-volatile solution may be detrimental [2–4]. Additionally, the molecular weight ( $M_w$ ) of the polymer and the concentration of the polymer in the solution are key factors that govern the degree of polymer chain entanglement, which in turn affects the solution's viscosity and the quality of the electrospun fibers [5].

The fabrication of fibers relies on the equilibrium of forces resulting from surface tension, the concentration of charges on the jet, and the viscosity of the solution. The viscosity ( $\eta$ ) and molecular weight of the polymer are directly related, and their relationship is expressed in the form of the Mark–Houwink Equation [6,7]

$$[\eta] = K \cdot M_w^\alpha$$

where  $\alpha$  and  $K$  are constants for a given polymer, solvent, and temperature.

Surface tension causes the liquid jet to transform into one or multiple spherical droplets in order to minimize surface area due to Rayleigh instability [8]. On the other hand, the electrostatic repulsion between charges on the jet counteracts this effect and promotes an increase in surface area, leading to the creation of a thin jet. The viscoelastic forces present in a polymer solution also play a vital role in bead-free fiber fabrication, as they prevent changes in shape and help create fibers. By adjusting the interplay between these forces, various fiber structures can be produced. For instance, by strengthening the impact of viscoelastic and charge repulsion forces compared to surface tension, it is possible to prevent the formation of beads. While the impact of solution concentration on fiber structure is widely known, it is the alteration in solution viscosity that ultimately leads to changes in the morphology of electrospun fibers [9].

Electrospinning fibers from polymers with lower molecular weights ( $M_w$ ) presents significant challenges due to the inherent physical properties of these materials. High-molecular-weight polymers are typically favored in electrospinning because they offer the necessary chain entanglement that facilitates fiber formation. In contrast, when using

polymers with lower  $M_w$ , the surface tension of the polymer solution often exceeds its viscoelastic forces. This imbalance results in the formation of beads along the fibers, which is an undesirable outcome. Beads within the fiber structure can significantly impair the mechanical integrity and functional performance of the resultant fiber mat, as they act as sites of structural weakness and/or defects. To mitigate this issue and achieve a uniform, beadless fiber morphology, careful optimization of electrospinning parameters is essential. This includes adjusting the solution concentration, as well as the electrospinning voltage, flow rate, and distance between the needle and collector. Achieving the optimal set of conditions is crucial to produce defect-free electrospun fibers, which is vital for their application in fields where high performance and consistency of physical properties are imperative.

Polyvinylpyrrolidone (PVP) is a versatile synthetic polymer, denoted by the molecular formula  $(C_6H_9NO)_n$ . The ball-and-stick model presented in Figure 2 illustrates the molecular composition of PVP. This polymer has been extensively combined with materials such as titanium dioxide ( $TiO_2$ ), Titanium nitride (TiN), and carbon nanotubes (CNTs) to explore its potential in sensing technologies [10–12]. The biocompatibility and nontoxicity of PVP also make it a popular choice in the field of drug delivery systems [13,14].

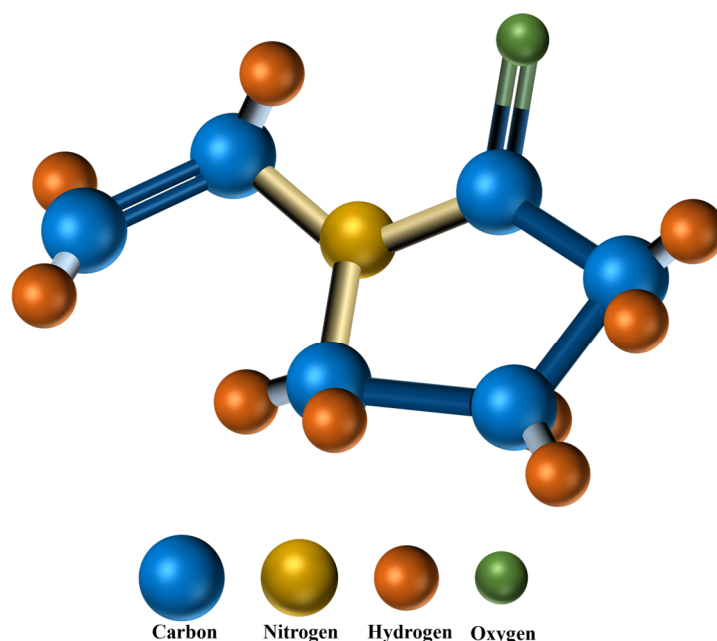


**Figure 2.** Ball-and-stick model of PVP molecular structure.

Commercially, PVP is available in a spectrum of molecular weights ( $M_w$ ), but it is commonly utilized at  $M_w \geq 130,000$  g/mol for various applications. Recent research has highlighted how different electrospinning parameters affect the morphology of PVP fibers, with these studies typically using a molecular weight of 130,000 g/mol as a standard [15–19]. However, there is a noticeable gap in the literature regarding the systematic exploration of electrospun PVP fibers at lower molecular weights.

Addressing this research gap could reveal significant insights into the fundamentals of electrospinning PVP. By tailoring the solution concentration (expressed in weight percent, wt%) for lower molecular weights, it may be possible to produce thinner fibers. These finer fibers can have the potential to enhance performance across a range of applications due to their increased surface area and unique physical properties. Therefore, further investigation into the optimization of electrospinning parameters for PVP with lower molecular weights is not only warranted but could also open new avenues for material innovation.

In bridging the current knowledge gap, this study offers a significant exploration of the electrospinning process using lower molecular weight Polyvinylpyrrolidone (PVP) variants,

specifically 10,000 and 55,000 g/mol. Through careful optimization of the solution concentration (wt%) and electrospinning parameters, we have successfully fabricated uniform electrospun fibers. Additionally, this study provides insight into the effects of needle gauge size and the distance from the needle tip to the collector (NCD) on the fiber morphology. Our findings elucidate crucial electrospinning process parameters that markedly influence fiber fabrication, particularly for polymers with lower molecular weights. This research not only advances our fundamental understanding of electrospinning dynamics but also paves the way for innovative applications of fine-tuned nanofibrous materials.

## 2. Experimental Details

### 2.1. Materials

Polyvinylpyrrolidone (PVP) possessing  $M_w$  10,000 g/mol and 55,000 g/mol, as well as solvent Ethanol (purity 99.9%), were purchased from Sigma Aldrich (St. Louis, MO, USA) to carry out the experimental work.

### 2.2. Parameter Optimization for PVP ( $M_w \sim 10,000$ g/mol and 55,000 g/mol)

Polyvinylpyrrolidone (PVP) exhibits solubility in a wide range of organic solvents as well as deionized water. In this study, ethanol was employed as a solvent for the preparation of the PVP polymer solution. This choice was made due to the higher evaporation rate of the PVP solution at ambient temperature. Polymer solutions of PVP with varying molecular weights were formulated at concentrations of 10 wt%, 30 wt%, and 50 wt%. It is noteworthy that wt% denotes the ratio of the mass of PVP to the mass of ethanol  $\times 100$ . To ensure uniformity, the solutions underwent magnetic stirring for one hour at room temperature. Subsequently, the solutions were loaded into a 10 mL syringe connected to a flow meter/syringe pump (1000-US/SyringeONE, New Era Pump Systems Inc., Farmingdale, NY, USA) for the electrospinning process. The process parameters utilized for electrospinning are detailed in Table 1.

**Table 1.** Electrospinning process parameters used for different concentrations of PVP<sub>10000</sub> and PVP<sub>55000</sub>.

Process Parameters	10 wt%	30 wt%	50 wt%
Needle Gauge (G)	25 (inner diameter: 0.260 mm)	25 (inner diameter: 0.260 mm)	25 (inner diameter: 0.260 mm)
NCD (cm)	14	14	14
Voltage (kV)	15, 20, 25	15, 20, 25	15, 20, 25
Flow rate (mL/h)	0.5, 1.0 (both flow rates at each voltage)	0.5, 1.0 (both flow rates at each voltage)	0.5, 1.0 (both flow rates at each)

### 2.3. Effect of Variation in Needle Gauge and Needle Tip-to-Collector Distance

In this phase of the experimental investigation, a consistent flow rate of 0.5 mL/h and an applied voltage of 20 kV were maintained for all samples. The 25G needle, with an inner diameter (ID) of 0.260 mm, was substituted with a 22G needle (ID~0.413 mm), while the distance between the needle and collector was adjusted within the range of 12–16 cm. Spinning solutions of 80 wt% PVP<sub>10000</sub> and 50 wt% PVP<sub>55000</sub> were employed for the experimental procedures. The deposition duration for each sample was controlled within an interval of 5–10 min. Electrospinning parameters used in this part of the experimental work are tabulated in Table 2.

**Table 2.** Electrospinning process parameters used to study the effect of needle gauge and needle-to-collector distance (NCD) on fiber morphology.

Solution wt%	Needle Gauge (G)	NCD (cm)	Voltage (kV)	Flow Rate (mL/h)
PVP <sub>55000</sub> 50 wt%	22 (ID: 0.413 mm)	12, 14, 16	20	0.5
PVP <sub>10000</sub> 80 wt%	22 (ID: 0.413 mm)	12, 14, 16	20	0.5

#### 2.4. Characterization

The morphology of the samples was analyzed using scanning electron microscopy (Zeiss Merlin). ImageJ software (<https://imagej.net/ij/>) was utilized to estimate the fiber diameter from SEM images, with 40 fibers examined for each sample to investigate the impact of process parameters on morphology. The diameter distribution of all samples was further analyzed using OriginPro 2024.

### 3. Results and Discussion

The results section will be subdivided into three parts, discussing the parameter optimization for PVP<sub>10000</sub> and PVP<sub>55000</sub>, as well as the effect of variation in needle gauge and NCD.

#### 3.1. Parameter Optimization for PVP<sub>10000</sub>

In the electrospinning experiments conducted at room temperature, three PVP<sub>10000</sub> solutions with concentrations of 10 wt%, 30 wt%, and 50 wt% were utilized, adhering to the process parameters delineated in the experimental section. Subsequent SEM analysis was performed on the derived samples. As depicted in Figure S1, the samples generated from the 10 wt% solution did not yield fibers; instead, particle formation was observed across all tested voltages and flow rates. This outcome is attributed to the low polymer concentration, which is hypothesized to increase the surface tension and reduce the solution's viscosity, thereby inhibiting the elongation necessary for fiber formation. Further investigation into the relationship between polymer concentration, surface tension, and viscosity is warranted to substantiate this hypothesis and refine the electrospinning process parameters for low-concentration solutions.

The concentration of PVP<sub>10000</sub> was increased to 30 wt% and 50 wt%. While fibers tended to form, particle formation was significantly higher than fibers. These results indicate that increasing the polymer concentration leads to an increase in the viscosity and viscoelasticity of the solution. This increase overcomes the surface tension of the solution, allowing fiber fabrication to occur. SEM micrographs of these samples are shown in Figures 3 and 4.

Higher concentrations of PVP<sub>10000</sub> increased the viscosity of the spinning solution, but the spinnability remained low. In the 30 wt% solution, fibers tended to form at a higher flow rate of 1.0 mL/h at 20 kV (Figure 3). However, with the 50 wt% spinning solution, a lower flow rate of 0.5 mL/h showed a higher fiber density (Figure 4).

Particle density remained high for all voltages at both flow rates, prompting an increase in PVP<sub>10000</sub> concentration to 70 wt%. Figure 5 illustrates SEM micrographs and their respective fiber diameter distribution curves.

Considering the increase in fiber density at a lower flow rate for the 50 wt% spinning solution, electrospinning of the 70 wt% spinning solution was conducted at 0.5 mL/h, with other process parameters unchanged. This solution exhibited a higher fiber density and lower bead density. Increasing the voltage reduced bead formation, but it was not raised above 25 kV to prevent instability of the Taylor cone [20] and to ensure a uniform fiber diameter distribution. Analysis of fiber diameter distribution revealed that higher voltages resulted in smaller average fiber diameters. The average diameter of all samples was below 0.300  $\mu\text{m}$ , indicating enhanced uniformity with increasing voltage. The better uniformity of the fiber diameter depicted the stabilization of the Taylor cone at higher voltages, which led to uniform stretching of the fiber jet. Average diameters were observed

to be  $0.270 \pm 0.086 \mu\text{m}$ ,  $0.233 \pm 0.079 \mu\text{m}$ , and  $0.255 \pm 0.063 \mu\text{m}$  for 15 kV, 20 kV, and 25 kV applied voltages, respectively. The decrease in fiber diameter at 20 kV suggests that the higher charge density assisted in stretching the fiber jet. However, at 25 kV, the fiber diameter tends to increase, which is attributed to higher solution ejection from the needle tip due to increased applied voltage [21]. No particle formation was observed for these samples at any voltage. Moreover, the higher PVP<sub>10000</sub> concentration led to increased viscoelasticity and spinnability of the solution.

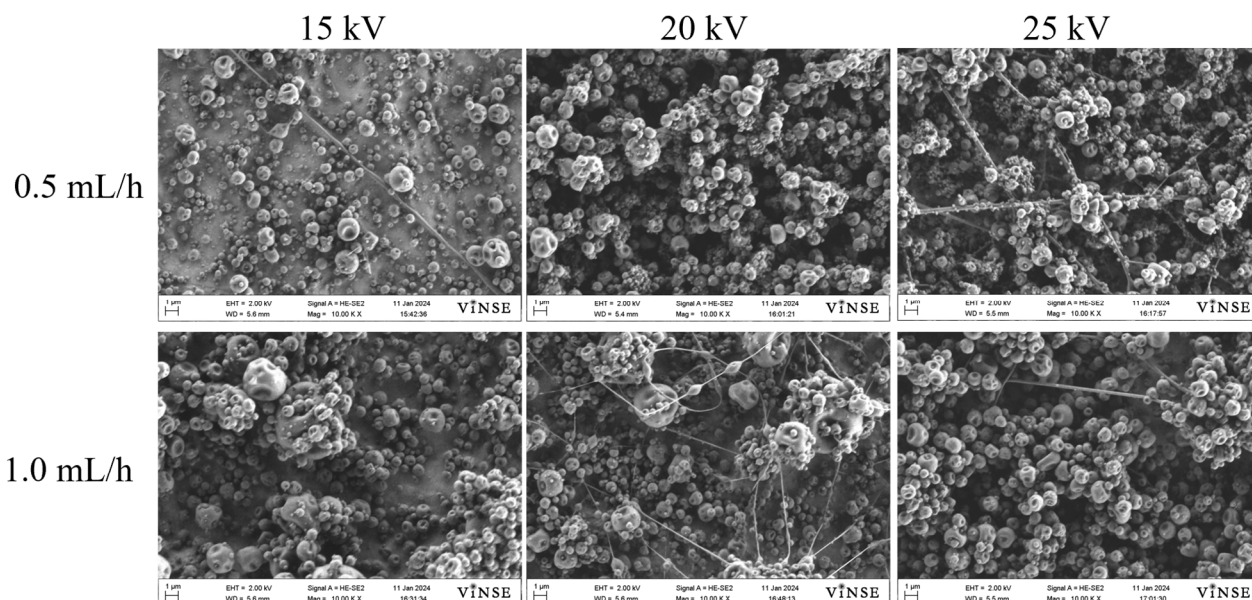


**Figure 3.** SEM micrographs of samples prepared using 30 wt% PVP<sub>10000</sub> solution at 14 cm NCD.

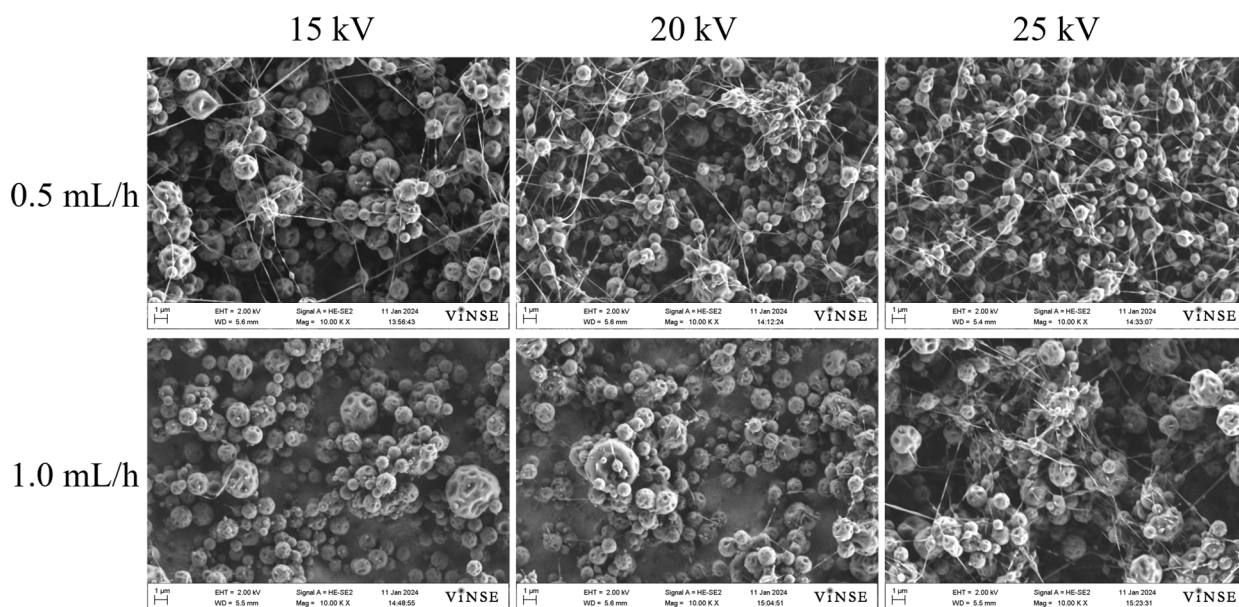


**Figure 4.** SEM micrographs of samples prepared using 50 wt% PVP<sub>10000</sub> solution at 14 cm NCD.

To completely avoid bead formation, the PVP<sub>10000</sub> concentration was increased to 80 wt%. SEM results revealed no bead formation for any of these samples (Figure 6).

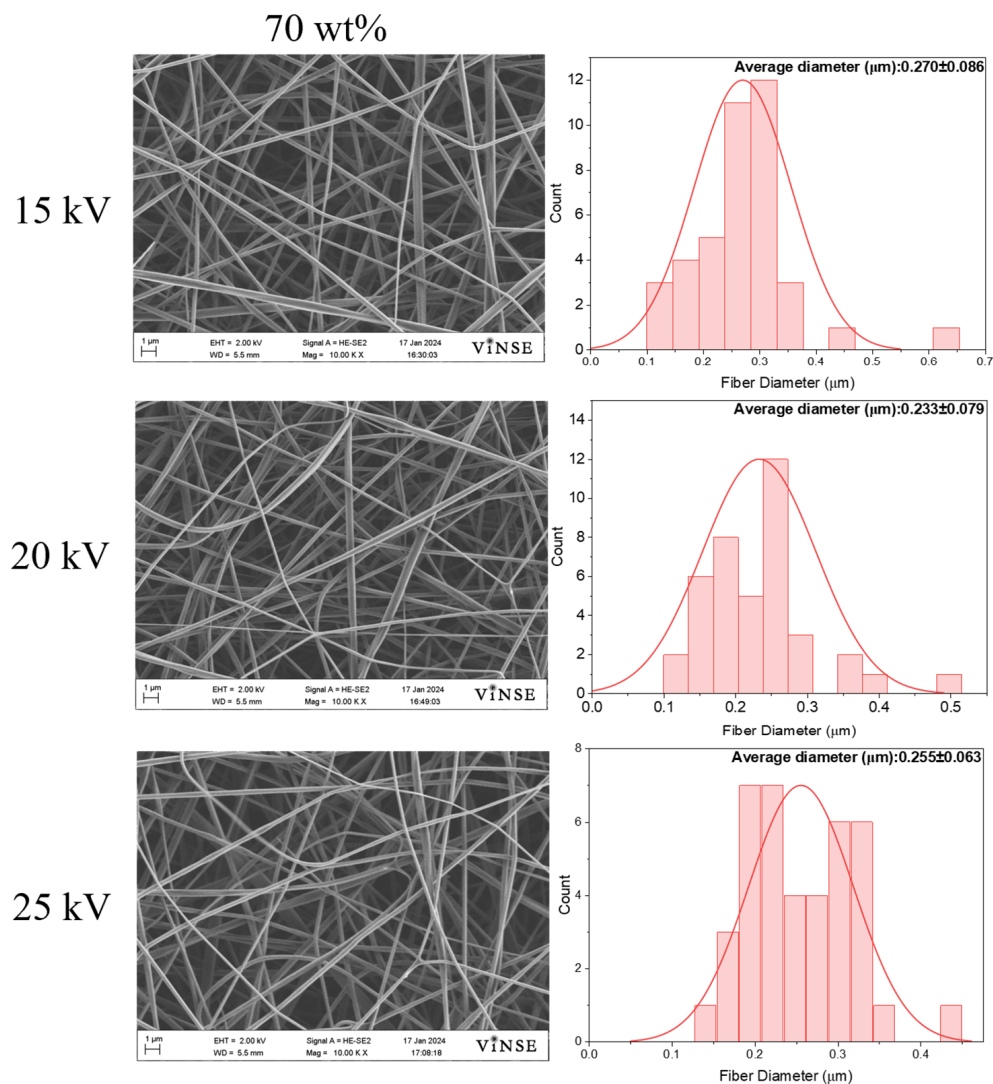


**Figure 5.** SEM micrographs and fiber diameter distribution graphs of samples prepared with 70 wt% PVP<sub>10000</sub> solution at 14 cm NCD and 0.5 mL/h flow rate.

This solution concentration (80 wt%) was opted to be the optimized wt% for PVP<sub>10000</sub>. The surface tension was completely overcome by the viscoelastic forces, which as a result produced fibers with fine morphology and no bead formation [22]. The fiber diameter was observed to decrease at 20 kV as compared to 15 kV; however, at 25 kV, it tended to increase. The increase in the average fiber diameter at a higher voltage is attributed to an increase in polymer solution extraction. It is worth mentioning that the increase in concentration from 70 wt% to 80 wt% led to an increase in the average fiber diameters at all applied voltages. Average diameters were  $0.370 \pm 0.111 \mu\text{m}$ ,  $0.245 \pm 0.083 \mu\text{m}$ , and  $0.330 \pm 0.129 \mu\text{m}$  for 15 kV, 20 kV, and 25 kV. The diameter distribution was observed to be uniform at 20 kV for both 70 wt% and 80 wt% concentrations. It was also concluded from these results that the fiber diameter tends to increase at higher polymer concentrations. No bead formation was observed for the 80 wt% PVP<sub>10000</sub> concentration. Therefore, the optimized parameters to prepare bead-free fibers using PVP<sub>10000</sub> were found to be 80 wt% concentration, 0.5 mL/h, and 20 kV applied voltage for 14 cm and 25G needle.

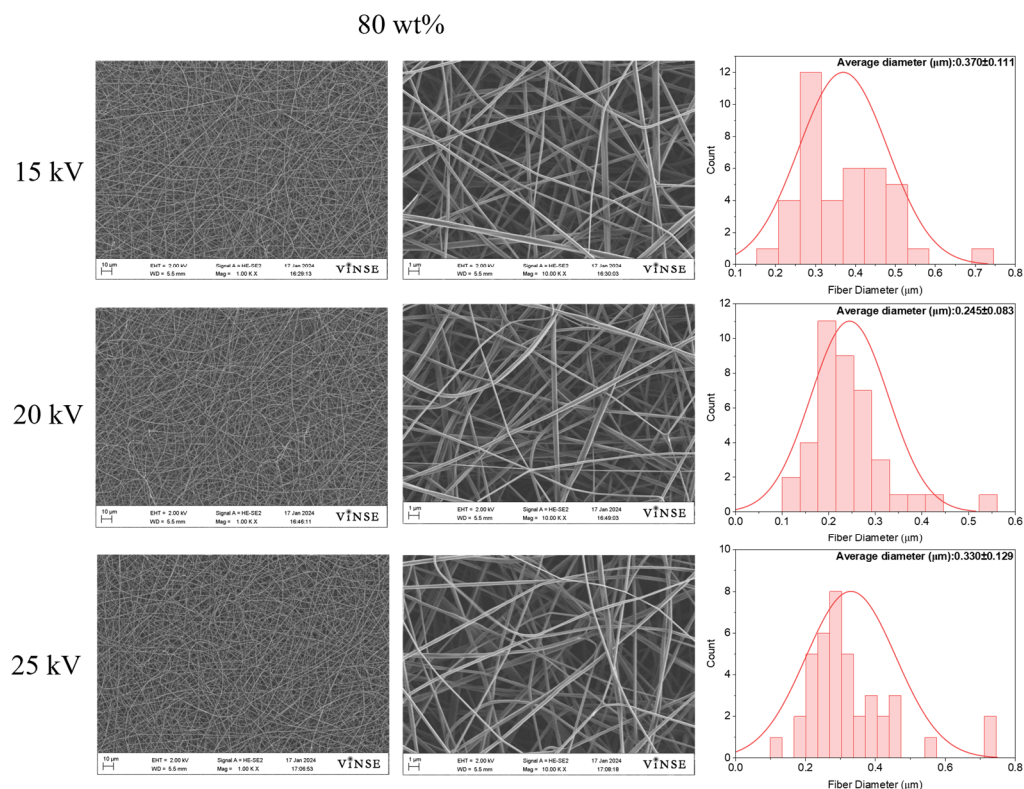


**Figure 6.** SEM micrographs and fiber diameter distribution graphs of samples prepared with 80 wt% PVP<sub>10000</sub> solution at 14 cm NCD and 0.5 mL/h flowrate.

### 3.2. Parameter Optimization for PVP<sub>55000</sub>

As previously mentioned, spinning solutions with concentrations of 10 wt%, 30 wt%, and 50 wt% were prepared using PVP<sub>55000</sub>. The representative SEM micrographs for the 10 wt% PVP<sub>55000</sub> concentration are displayed in Figure S2. No fiber formation was observed at any voltage or flow rate for this concentration due to the very low viscosity of the solution. In Figure 7, SEM micrographs of samples prepared using a 30 wt% PVP<sub>55000</sub> solution at 15 kV, 20 kV, and 25 kV, with flow rates ranging from 0.5 mL/h to 1.0 mL/h, are shown.

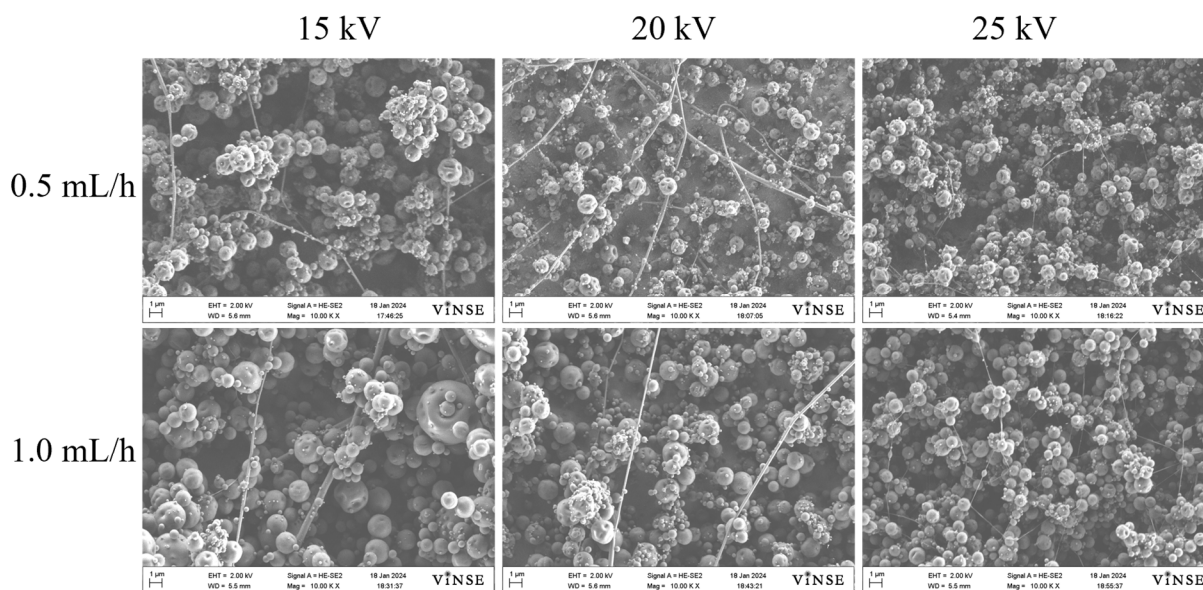


**Figure 7.** SEM micrographs of samples prepared with 30 wt% PVP<sub>55000</sub> solution at 14 cm NCD.

Compared to the 10 wt% PVP<sub>10000</sub> solution, these samples exhibited fiber fabrication; however, the particle density was still notably high in both cases. The fiber density for the 30 wt% PVP<sub>55000</sub> solution was highest at a flow rate of 0.5 mL/h and 20 kV. Upon increasing the concentration to 50 wt%, a smooth fiber morphology was observed at a flow rate of 0.5 mL/h, as depicted in Figure 8.

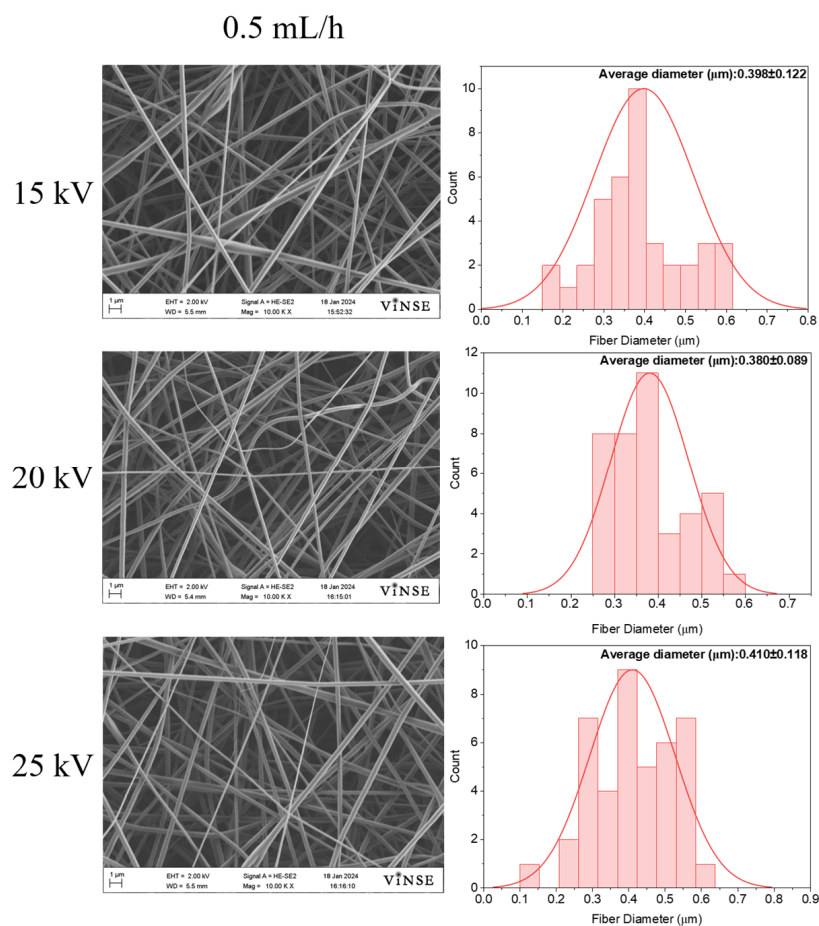


**Figure 8.** SEM micrographs of samples prepared using 50 wt% PVP<sub>55000</sub> at 14 cm NCD and 0.5 mL/h flow rate.

Bead formation was observed at lower voltages (15 kV) but not at higher voltages. The average fiber diameters for a flow rate of 0.5 mL/h were found to be  $0.398 \pm 0.122 \mu\text{m}$ ,  $0.380 \pm 0.089 \mu\text{m}$ , and  $0.410 \pm 0.118 \mu\text{m}$  for applied voltages of 15 kV, 20 kV, and 25 kV, respectively.

To understand the effect of flow rate on fiber morphology, the flow rate was increased from 0.5 mL/h to 1.0 mL/h. Figure 9 shows the SEM micrographs and their corresponding diameter distributions for these samples.

The diameter of the fibers exhibited an increase when subjected to a higher flow rate of 1.0 mL/h at 15 kV, resulting in a measurement of  $0.513 \pm 0.175 \mu\text{m}$ . Additionally, the occurrence of bead formation was noted at the higher flow rate. The elevated flow rate causes the generation of larger droplets at the needle tip, with the charge applied to the droplets being insufficient to counteract the surface tension, thereby leading to the formation of beads. It tended to decrease at 20 kV applied voltage and increase at 25 kV (Figure 10).

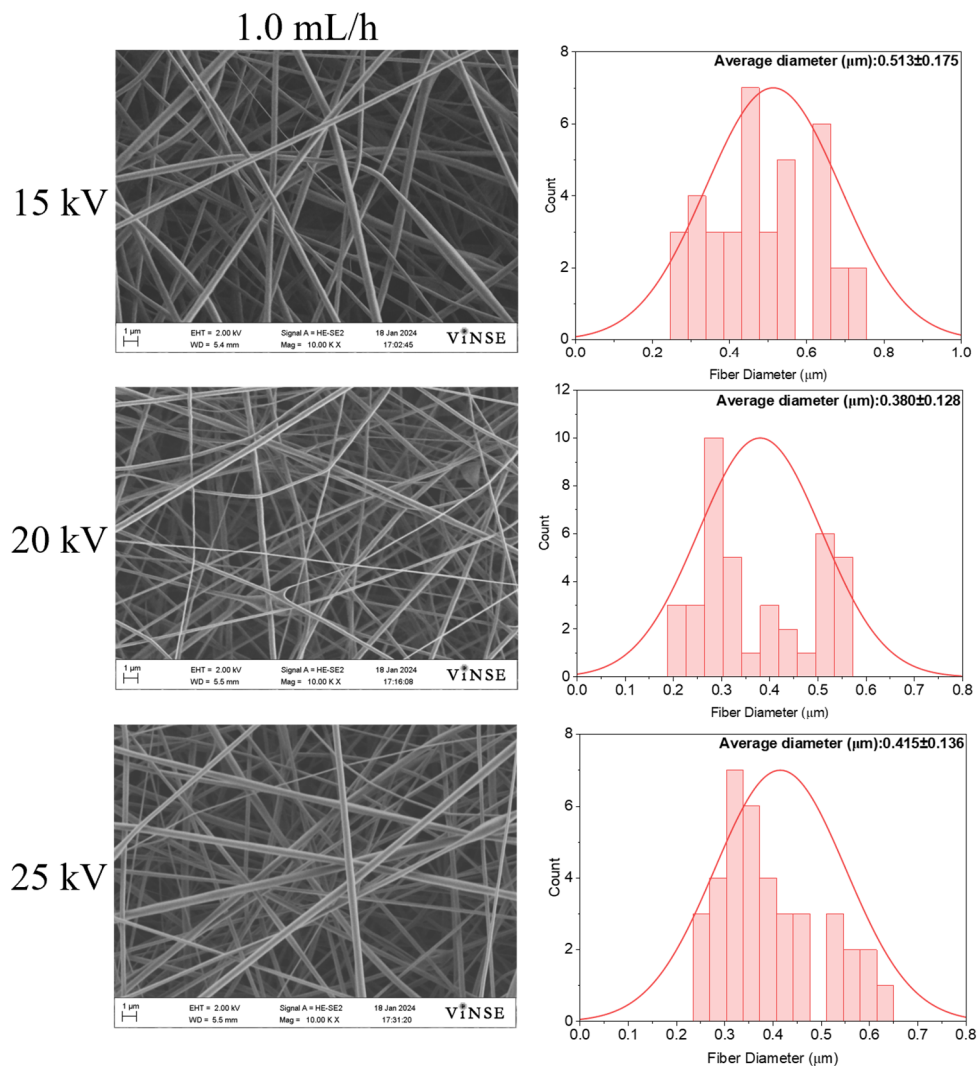


Figure 9. SEM micrographs of samples prepared using 50 wt% PVP<sub>55000</sub> at 14 cm NCD and 1.0 mL/h flow rate.

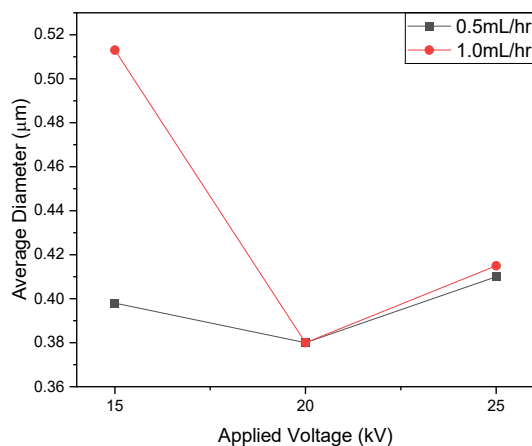
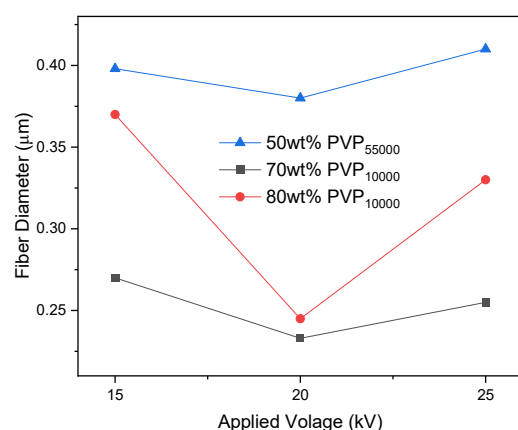


Figure 10. Graphical representation for the effect of flow rate on average fiber diameter; samples prepared using 50 wt% PVP<sub>55000</sub>, 14 cm NCD, and 25G needle.

The increase in polymer solution extraction at 25 kV, combined with a higher flow rate, resulted in greater bead formation at the higher voltage. Additionally, the diameter distribution was observed to increase with the flow rate. The optimized parameters for

PVP<sub>55000</sub> fiber fabrication were determined to be 50 wt% polymer concentration, 0.5 mL/h flow rate, and 20 kV applied voltage for 14 cm NCD and 25 gauge needle.

Considering the SEM analysis of the fibers prepared by spinning 50 wt% solutions of both PVP<sub>10000</sub> and PVP<sub>55000</sub>, it is concluded that a higher molecular weight significantly assisted in fiber fabrication. A molecular weight of 55,000 g/mol exceeds the critical entanglement molecular weight (generally in the range of 10,000–20,000 g/mol), which drastically increases the viscosity of the solution. Hence, fiber formation is observed for 50 wt% PVP<sub>55000</sub>; however, same is not true for PVP<sub>10000</sub> [23]. However, increasing the concentration also leads to an increase in entanglement [24]; therefore, 70 wt% and 80 wt% PVP<sub>10000</sub> exhibited fiber fabrication, as previously discussed. The fiber diameter of the samples prepared using 50 wt% PVP<sub>55000</sub> was still higher. From detailed diameter analysis, it was also revealed that the higher molecular weight (55,000 g/mol in this case) assisted in the fabrication of fibers with higher diameters, even at lower concentrations. Figure 11 illustrates the fiber diameter plots at different concentrations of PVP<sub>10000</sub> (70 wt% and 80 wt%) and PVP<sub>55000</sub> (50 wt%).



**Figure 11.** Graphical representation depicts variation in average diameter as a function of applied voltage for samples prepared at 0.5 mL/h using different concentrations (wt%) and PVP molecular weights.

### 3.3. Effect of Needle Gauge and NCD

As mentioned earlier, the needle gauge was changed to 22G for optimized electrospinning process parameters (deduced from the results discussed above) and solution concentrations of 80 wt% PVP<sub>10000</sub> and 50 wt% PVP<sub>55000</sub>. The needle tip-to-collector distance (NCD) was varied between 12 cm and 16 cm to observe the variation in fiber morphology.

Figure 12 shows the SEM images and their corresponding diameter distributions for the samples prepared using 80 wt% PVP<sub>10000</sub> at three NCDs (12 cm, 14 cm, and 16 cm) at 20 kV and 0.5 mL/h, using a 22G needle.

Average diameters were observed to be  $0.349 \pm 0.118 \mu\text{m}$ ,  $0.297 \pm 0.089 \mu\text{m}$ , and  $0.341 \pm 0.091 \mu\text{m}$  for 12 cm, 14 cm, and 16 cm NCD, respectively. It was observed that by increasing the distance from 12 cm to 14 cm, the fiber diameter tended to decrease. This trend is associated with the stretching of the fiber jet for longer NCD, which led to the decrease in the fiber diameter. However, at 16 cm, the fiber diameter increased to  $0.341 \pm 0.091 \mu\text{m}$ , indicating that the electrostatic force due to the applied voltage (20 kV) for this distance did not suffice to stretch the jet enough to decrease the fiber diameter [25,26]. No bead formation was observed at any distance. The diameter distribution became narrower with an increase in distance, indicating a better uniformity of the fiber diameter. The most uniform fiber diameter deposition was observed for samples prepared at 14 cm. As compared to fibers fabricated using identical process parameters for 25G and 14 cm NCD, the fiber diameter was observed to increase when a 22G needle was used. This

increase was attributed to the larger drop formed at the needle tip due to the increased needle diameter. The applied voltage was high enough to create a charge that overcame surface tension, along with the optimal viscoelasticity of the polymer solution, preventing bead formation.

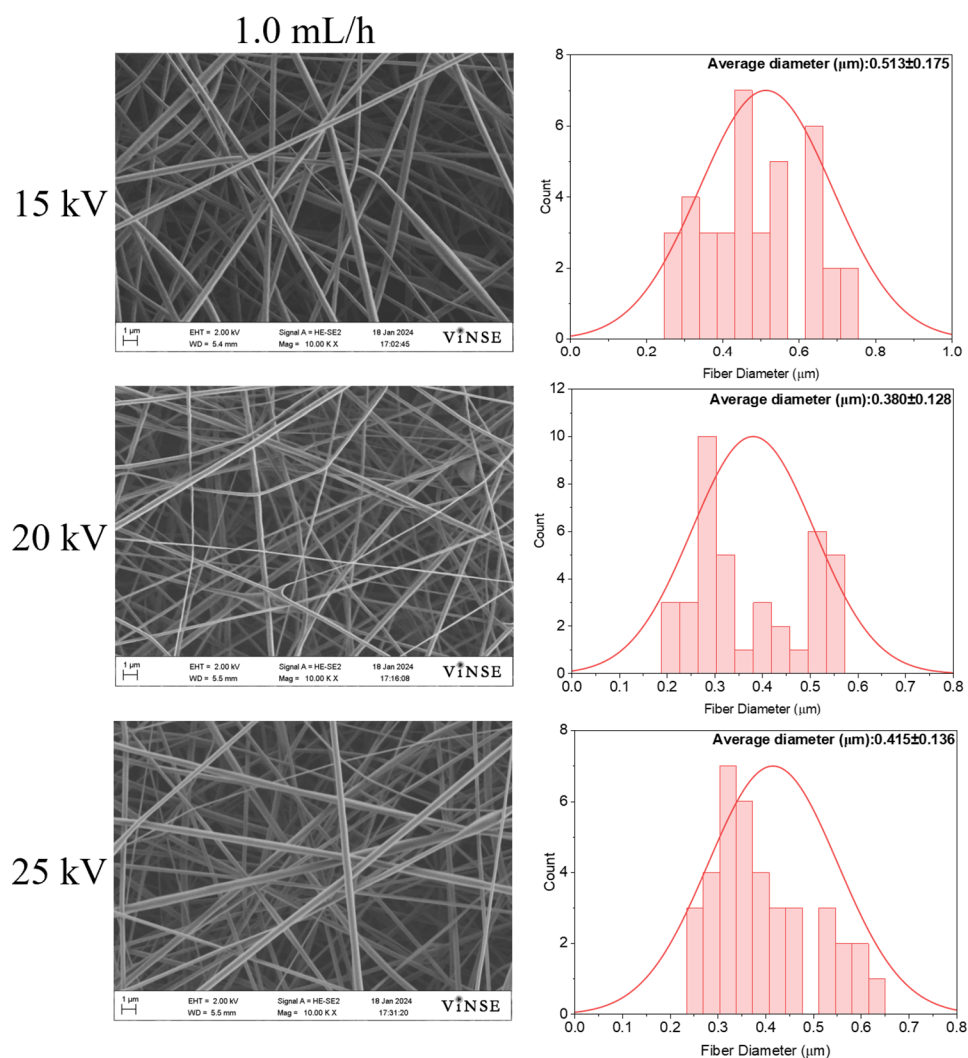


**Figure 12.** SEM micrographs of samples prepared using a 22G needle at 12 cm, 14 cm, and 16 cm at 20 kV, 0.5 mL/h, using 80 wt% PVP<sub>10000</sub>.

When the PVP<sub>55000</sub> solution was used for electrospinning using a 22G needle at different distances (12 cm, 14 cm, and 16 cm), a significantly high bead density was observed. The variation in distance or lower flow rate for this concentration did not assist in decreasing the bead formation. This occurred due to the wider diameter of the 22G needle (0.413 mm). The larger drop formation resisted the applied voltage to overcome the surface tension, which led to the formation of large beads. Given that the spinning solution demonstrated no bead density when electrospun with a 25G (0.260 mm) needle, it can be inferred that the solution parameters were suitable for this needle gauge. However, in order to prevent bead formation when utilizing a 22G needle, additional optimization of the solution concentration is necessary. It worth mentioning that the same results were observed for all the distances; therefore, the representative SEM micrographs for these samples have been shown in Figure 13. Increasing the concentration of PVP<sub>55000</sub> may lead to a decrease in bead formation when using a smaller needle gauge.

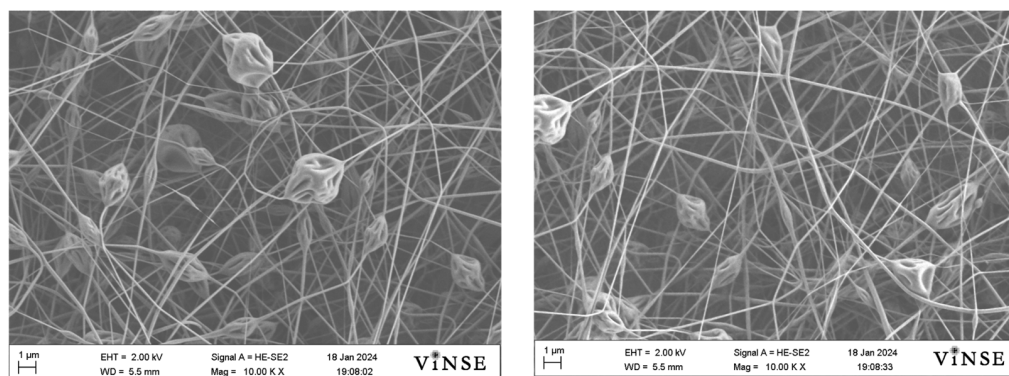


**Figure 13.** Representative SEM micrographs of samples prepared using a 22G needle, 0.5 mL/h, 20 kV with 50 wt% PVP<sub>55000</sub>.

#### 4. Conclusions

This study successfully optimized the process parameters for producing electrospun fibers of PVP with lower molecular weights of 10,000 g/mol and 55,000 g/mol. It was found that a polymer with a lower molecular weight necessitates a higher polymer concentration to achieve the optimal viscosity for fiber production. Fiber ejection depends significantly on the higher viscoelasticity of the solution; therefore, preparation of the solution is a crucial step to prepare smooth, bead-free fibers. Moreover, it was observed that an increase in flow rate can lead to an increase in fiber diameter; however, the influence of flow rate at higher voltages is negligible. If the viscoelasticity of the solution and the applied charge density on the solution drop are not high enough to overcome the surface tension, bead formation is observed, especially at a higher flow rate, as observed for 50 wt% PVP<sub>55000</sub>. Same observation was made when the needle gauge was reduced (the inner diameter of the needle increased). To prepare thinner fibers, a lower molecular weight is observed to be ideal. There are some polymers that hold great potential for drug delivery; however, their lower molecular weights hinder the fiber formation. The main objective of this research was to enhance the electrospinning process conditions in order to produce smooth bead-free fibers using a polymer with a lower molecular weight. It can be inferred that this objective has been successfully met. Another aim of this study was to explore the underlying principles of the electrospinning process variables that influence fiber morphology. This research effectively examined the combined and individual impacts of various electrospinning process parameters on the fiber structure. The findings of this study will aid in comprehending the basic principles necessary to optimize process parameters for the creation of fibers from these types of polymers.

#### 5. Future Work

A thorough investigation will be conducted to analyze and correlate the viscosity of the spinning solution (as a function of concentration and molecular weight) in a systematic manner. To further investigate how different electrospinning process parameters impact composite formation, the plan is to encapsulate carbon nanotubes (CNTs) within PVP fibers using a uniaxial electrospinning system. The study will aim to assess the potential of CNTs embedded in PVP fibers for microwave absorption applications. Additionally, the impact of using higher voltages (>25 kV) in producing PVP fibers and CNTs/PVP composite fibers will be examined to understand how voltage affects their morphology and, consequently, their transport properties (such as electrical and thermal characteristics). This fundamental research will also assist in optimizing process parameters for other polymers (like poly vinyl alcohol) with lower molecular weights that will be utilized in future studies.

**Supplementary Materials:** The following supporting information can be downloaded at <https://www.mdpi.com/article/10.3390/polym16091217/s1>, Figure S1: Representative SEM micrographs of the samples

prepared using 10 wt% spinning solution PVP<sub>10000</sub>. Figure S2: Representative SEM micrographs of the samples prepared using 10 wt% spinning solution PVP<sub>55000</sub>.

**Author Contributions:** Conceptualization, F.T.Z.; Methodology, F.T.Z. and A.O.A.; Validation, R.M.; Formal analysis, F.T.Z.; Investigation, F.T.Z.; Resources, Q.Q. and R.M.; Writing—original draft, F.T.Z.; Writing—review & editing, Y.Z., Q.Q. and R.M.; Supervision, R.M.; Project administration, R.M.; Funding acquisition, Q.Q. and R.M. All authors have read and agreed to the published version of the manuscript.

**Funding:** This research was funded by the NSF through the Partnership for Research and Education in Materials (PREM) program DMR-2122169, HBCU-RISE program HRD-1924241, and by NIH-funded Meharry-Vanderbilt-Tennessee State University Cancer Partnership U54CA163072.

**Institutional Review Board Statement:** Not Applicable.

**Data Availability Statement:** Data are contained within the article and Supplementary Materials.

**Acknowledgments:** James McBride at Vanderbilt Institute of Nanoscale Science and Engineering (VINSE) is acknowledged for his unwavering support in obtaining FESEM images.

**Conflicts of Interest:** There is no conflict to declare.

## References

- Haider, A.; Haider, S.; Kang, I.K. A comprehensive review summarizing the effect of electrospinning parameters and potential applications of nanofibers in biomedical and biotechnology. *Arab. J. Chem.* **2018**, *11*, 1165–1188. [[CrossRef](#)]
- Zahra, F.T.; Quick, Q.; Mu, R. Electrospun PVA Fibers for Drug Delivery: A Review. *Polymers* **2023**, *15*, 3837. [[CrossRef](#)]
- Williams, G.R.; Raimi-Abraham, B.T.; Luo, C.J. Nanofibres in Drug Delivery Applications. *Fibers* **2023**, *11*, 21. [[CrossRef](#)]
- Liu, G.; Gu, Z.; Hong, Y.; Cheng, L.; Li, C. Electrospun starch nanofibers: Recent advances, challenges, and strategies for potential pharmaceutical applications. *J. Control. Release* **2017**, *252*, 95–107. [[CrossRef](#)]
- Wei, Q.; Tao, D.; Xu, Y. 1—Nanofibers: Principles and manufacture. In *Functional Nanofibers and their Applications*; Wei, Q., Ed.; Woodhead Publishing: Sawston, UK, 2012; pp. 3–21. [[CrossRef](#)]
- Kwaambwa, H.M.; Goodwin, J.W.; Hughes, R.W.; Reynolds, P.A. Viscosity, molecular weight and concentration relationships at 298 K of low molecular weight cis-polyisoprene in a good solvent. *Colloids Surfaces A Physicochem. Eng. Asp.* **2007**, *294*, 14–19. [[CrossRef](#)]
- Marani, D.; Sudireddy, B.R.; Kiebach, W.-R.; Nielsen, L.; Ndoni, S. Rheological properties of poly(vinylpyrrolidone) as a function of molecular weight. *Nord. Rheol. Soc. Trans.* **2014**, *22*, 11–18.
- Fong, H.; Chun, I.; Reneker, D.H. Beaded nanofibers formed during electrospinning. *Polymer* **1999**, *40*, 4585–4592. [[CrossRef](#)]
- Nezarati, R.M.; Eifert, M.B.; Cosgriff-Hernandez, E. Effects of humidity and solution viscosity on electrospun fiber morphology. *Tissue Eng. Part C Methods* **2013**, *19*, 810–819. [[CrossRef](#)]
- Lv, J.; Gu, W.; Cui, X.; Dai, S.; Zhang, B.; Ji, G. Nanofiber network with adjustable nanostructure controlled by PVP content for an excellent microwave absorption. *Sci. Rep.* **2019**, *9*, 4271. [[CrossRef](#)]
- Wei, Y.; Shi, Y.; Zhang, X.; Jiang, Z.; Zhang, Y.; Zhang, L.; Zhang, J.; Gong, C. Electrospinning of lightweight TiN fibers with superior microwave absorption. *J. Mater. Sci. Mater. Electron.* **2019**, *30*, 14519–14527. [[CrossRef](#)]
- Yadav, M.; Singh, G.; Lata, S. Polyvinylpyrrolidone/TiO<sub>2</sub> composites' preparation via sol-gel procedure furthered with non-enzymatic glucose sensing and antibacterial effectiveness. *Environ. Sci. Pollut. Res. Int.* **2023**, *30*, 98563–98580. [[CrossRef](#)]
- Franco, P.; De Marco, I. The Use of Poly(N-vinyl pyrrolidone) in the Delivery of Drugs: A Review. *Polymers* **2020**, *12*, 1114. [[CrossRef](#)]
- Kurakula, M.; Rao, G.S.N.K. Pharmaceutical assessment of polyvinylpyrrolidone (PVP): As excipient from conventional to controlled delivery systems with a spotlight on COVID-19 inhibition. *J. Drug Deliv. Sci. Technol.* **2020**, *60*, 102046. [[CrossRef](#)]
- Utkarsh; Hegab, H.; Tariq, M.; Syed, N.A.; Rizvi, G.; Pop-Iliev, R. Towards Analysis and Optimization of Electrospun PVP (Polyvinylpyrrolidone) Nanofibers. *Adv. Polym. Technol.* **2020**, *2020*, 4090747. [[CrossRef](#)]
- Zhu, L.; Zhu, W.; Hu, X.; Lin, Y.; Machmudah, S.; Wahyudiono; Kanda, H.; Goto, M. PVP/Highly Dispersed AgNPs Nanofibers Using Ultrasonic-Assisted Electrospinning. *Polymers* **2022**, *14*, 599. [[CrossRef](#)]
- Hu, X.; He, J.; Zhu, L.; Machmudah, S.; Wahyudiono; Kanda, H.; Goto, M. Synthesis of Hollow PVP/Ag Nanoparticle Composite Fibers via Electrospinning under a Dense CO<sub>2</sub> Environment. *Polymers* **2022**, *14*, 89. [[CrossRef](#)]
- Wahyudiono; Machmudah, S.; Murakami, K.; Okubayashi, S.; Goto, M. Generation of PVP fibers by electrospinning in one-step process under high-pressure CO<sub>2</sub>. *Int. J. Ind. Chem.* **2013**, *4*, 4–9. [[CrossRef](#)]
- Andjani, D.; Sriyanti, I.; Fauzi, A.; Edikresnha, D.; Munir, M.M.; Khairurrijal. Fabrication of Polyvinylpyrrolidone Fibers by Means of Rotary Forcespinning Method. *IOP Conf. Ser. Mater. Sci. Eng.* **2018**, *367*, 012044. [[CrossRef](#)]
- Chan, K.H.K.; Kotaki, M. Fabrication and morphology control of poly(methyl methacrylate) hollow structures via coaxial electrospinning. *J. Appl. Polym. Sci.* **2009**, *111*, 408–416. [[CrossRef](#)]

21. Syed Bakar, S.S.; Foong, K.M.; Abdul Halif, N.; Yahud, S. Effect of solution concentration and applied voltage on electrospun polyacrylonitrile fibers. *IOP Conf. Ser. Mater. Sci. Eng.* **2019**, *701*, 012018. [[CrossRef](#)]
22. Khajavi, R.; Abbasipour, M. 5—Controlling nanofiber morphology by the electrospinning process. In *Electrospun Nanofibers*; Elsevier Ltd.: Amsterdam, The Netherlands, 2017. [[CrossRef](#)]
23. Kuo, C.J.; Lan, W.L. 5—Gel spinning of synthetic polymer fibres. In *Advances in Filament Yarn Spinning of Textiles and Polymers*; Woodhead Publishing Limited: Sawston, UK, 2014. [[CrossRef](#)]
24. Gupta, B.S.; Moghe, A.K. 2—Nanofiber structures for medical biotextiles. In *Biotextiles as Medical Implants*; King, M.W., Gupta, B.S., Guidoin, R., Eds.; Woodhead Publishing: Sawston, UK, 2013; pp. 48–90. [[CrossRef](#)]
25. Singh, Y.P.; Dasgupta, S.; Nayar, S.; Bhaskar, R. Optimization of electrospinning process & parameters for producing defect-free chitosan/polyethylene oxide nanofibers for bone tissue engineering. *J. Biomater. Sci. Polym. Ed.* **2020**, *31*, 781–803.
26. Henriques, C.; Vidinha, R.; Botequim, D.; Borges, J.P.; Silva, J.A.M.C. A systematic study of solution and processing parameters on nanofiber morphology using a new electrospinning apparatus. *J. Nanosci. Nanotechnol.* **2009**, *9*, 3535–3545. [[CrossRef](#)]

**Disclaimer/Publisher’s Note:** The statements, opinions and data contained in all publications are solely those of the individual author(s) and contributor(s) and not of MDPI and/or the editor(s). MDPI and/or the editor(s) disclaim responsibility for any injury to people or property resulting from any ideas, methods, instructions or products referred to in the content.